  Bull. Chem. Soc. Jpn., 59, 3405—3415 (1986)

Fluorescence and Nonradiative Relaxation from Vibronic Levels of S_1 Pyrimidine: Effects of Molecular Rotation and Intramolecular Vibrational Redistribution

Osamu Sekiguchi,† Nobuhiro Ohta, and Hiroaki Baba*
Division of Chemistry, Research Institute of Applied Electricity, Hokkaido University, Sapporo 060
(Received May 19, 1986)

Emission characteristics of pyrimidine vapor which were measured after excitation into various S_1 vibronic levels with relatively low excess vibrational energies (ΔE) below 2650 cm^{-1} were found to depend markedly upon ΔE. The emission from a vibronic level with $\Delta E<1000$ cm^{-1} (e.g., $6a^1$ or 1^1) is sharp and attributable to the fluorescence from the initially prepared vibronic level (IPL), and that from a vibronic level with $\Delta E>1000$ cm^{-1} (e.g., 12^1, $6a^2$, or 12^2) involves broad fluorescence besides the IPL fluorescence. At low pressure, the broad fluorescence consists of fast and slow components with lifetimes comparable to those for the corresponding components of the IPL fluorescence. The broad fluorescence exhibits another slow component which is characterized by a less tendency to undergo collisional quenching. The quantum yield of the slow component of the IPL fluorescence clearly depends upon molecular rotation, whereas that of the broad fluorescence appears to show little or no rotational-level dependence. On the basis of these observations, the broad fluorescence is assigned to the one originating from S_1 vibronic levels that can be reached directly from the IPL through intramolecular vibrational redistribution (IVR) or indirectly via triplet levels. There exists no evidence to show that the IVR is affected by molecular rotation.

When an isolated molecule is optically excited, the excitation energy may be transferred nonradiatively from the initially prepared vibronic level to the other isoenergetic levels through redistribution of the vibrational energy.[1-4] Understanding of this sort of intramolecular vibrational redistribution (IVR) is important not only in elucidating intramolecular dynamics but also in exploring the possibility of state selective chemistry. The IVR phenomena have been investigated extensively within the first excited singlet state (S_1) under bulk gas conditions at room temperature or ultracold supersonic jet conditions.[3,4] Most of these investigations were performed with aromatic hydrocarbons and their alkyl or halogen derivatives,[3,4] all of which belong to the statistical limit case in radiationless electronic relaxation.

The IVR process is known to occur usually at vibronic levels with relatively high excess vibrational energies, ΔE. Thus, IVR occurs at $\Delta E=3000$ cm^{-1} in benzene itself[5] and at $\Delta E=2000$ cm^{-1} in *p*-difluorobenzene and *p*-fluorotoluene,[6] though IVR can be recognized at a small ΔE value of 530 cm^{-1} in substituted benzenes with a long side chain.[4,7] The times required for IVR range from sub-picosecond to microsecond, but those reported in recent papers are mostly of the order of picosecond.[8] The anharmonic interaction is considered to induce IVR, but the Coriolis coupling is sometimes regarded as responsible for IVR. Recently, Riedle et al. showed that the Coriolis coupling plays an important role in IVR in the third channel region of benzene.[9]

Pyrimidine is known to have an intermediate-case level structure and gives fast and slow components of fluorescence under collision-free conditions.[10,11] It has been established that, so far as the fluorescence resulting from excitation at the 0–0 absorption band or a lower vibronic band is concerned, the characteristics of the slow fluorescence component of an intermediate-case molecule undergo considerable variation across the rotational contour.[12-15] On the other hand, little attention has been directed to IVR in the intermediate-case molecules except for the work by Lim and his collaborators, who observed the IVR induced by excitation at the 12_0^2 absorption band of pyrimidine.[16]

In the present study, fluorescence and nonradiative relaxation in pyrimidine vapor have been observed after exciting the molecule into various S_1 vibronic levels with relatively low excess vibrational energies ranging from 600 to 2650 cm^{-1}. The purpose of the study is twofold. First, attention is given to the change in the effect of molecular rotation on electronic or vibrational relaxation with excess energy. Second, an attempt is made to elucidate the kinetic mechanism of the occurrence of IVR. It will be shown in this paper that, in the case of pyrimidine, IVR appears to take place at vibronic levels whose energies are much lower than usually expected.

Experimental

Pyrimidine obtained from Aldrich Chemical Co. was purified by repeated vacuum sublimation. Commercially available sulfur hexafluoride (SF_6) from Seitetsu Chemicals was used as an inert foreign gas without further purification. The pressure of pyrimidine was determined by measuring the absorption intensity or by using a capacitance manometer (MKS Baratron type 170).

All the optical measurements were carried out at room temperature. Absorption and fluorescence spectra, fluores-

† Present address: Department of Industrial Chemistry, Faculty of Engineering, Shinshu University, Nagano 380.

cence excitation spectra, and fluorescence decays were measured with a laser spectrophotometric system.[17] The procedures for these measurements are essentially the same as those reported in previous papers.[13,17] In the spectrophotometric system, a pulsed dye laser (Molectron DL 14) is pumped by a nitrogen laser (Molectron UV 22). The frequency of the dye laser is doubled by a KDP crystal to generate UV laser pulses, which are used for exciting the sample. The UV laser pulses have a linewidth of 0.5 cm^{-1} and a duration of 3 ns. Emission measurements were made with a 3.5 cm cubic quartz cell. Absorption spectra and fluorescence-excitation spectra were measured simultaneously. The excitation spectra were obtained by monitoring the fluorescence emission dispersed by a grating monochromator (Nikon G250) and were corrected for fluctuation of the laser intensity. A relative quantum yield spectrum is derived as a ratio of a corrected excitation spectrum to the corresponding absorption spectrum. No correction was made for the spectral sensitivity of the detecting system. Fluorescence decays were measured with a single photon counting lifetime apparatus equipped with a time-to-amplitude converter. The lifetimes of the fast fluorescence of pyrimidine were determined by the convolution method.

Results

The emission spectrum of pyrimidine vapor changes markedly in shape with the excess vibrational energy (ΔE) of the S_1 vibronic level excited. Figure 1 shows the emission spectra from 0^0, $6a^2$, and $6a^1 12^2$ levels of S_1 pyrimidine at a low pressure of 80.8 mTorr.† See Table 1 for the values of ΔE for the individual levels.[18,19] When ΔE is small (Fig. 1(a)), the emission spectrum consists of sharp fluorescence bands which are due to vibronic transitions starting from the initially prepared vibronic level (IPL). As ΔE increases, the intensity of the IPL fluorescence decreases, and a broad, structureless emission appears instead at longer wavelengths (Fig. 1(b)). From now on, the latter emission will be referred to as "broad fluorescence." It is seen in Fig. 1(c) that the emission from the $6a^1 12^2$ level having a large ΔE value consists almost solely of the broad fluorescence.

Thus, according to the results of the present study, the fluorescence from vibronic levels with $\Delta E<1000$ cm^{-1} is attributable solely to the IPL fluorescence, while that from vibronic levels with $\Delta E>1000$ cm^{-1} involves the broad fluorescence in addition to the IPL fluorescence. The features of the fluorescence and nonradiative relaxation from some representative vibronic levels in S_1 pyrimidine will be described in the following.

$6a^1$ Level (ΔE=613 cm^{-1}) and 1^1 Level (ΔE=941 cm^{-1}). Absorption, fluorescence excitation, and fluorescence quantum yield spectra at a low pressure are shown in Fig. 2(a) for the rotational contour of the $6a_0^1$ absorption band. It was found that the excitation spectrum does not change in shape and position with the fluorescence band monitored. The quantum yield

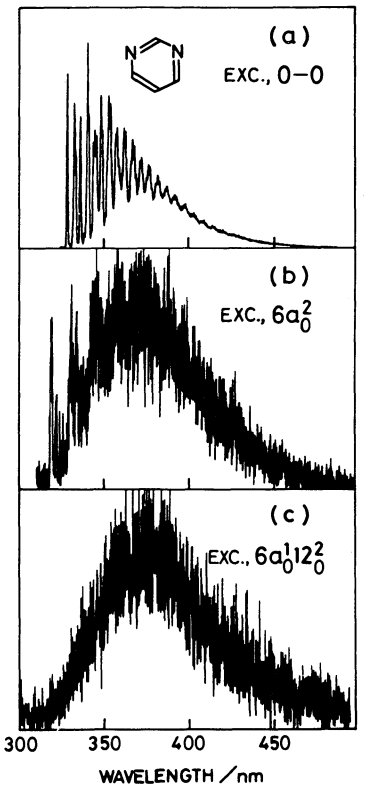

Fig. 1. Emission spectra of pyrimidine at 80.8 mTorr. Excitation bands: (a) 0—0; (b) $6a_0^2$; (c) $6a_0^1 12_0^2$. Spectral resolution is 0.6 nm in every case.

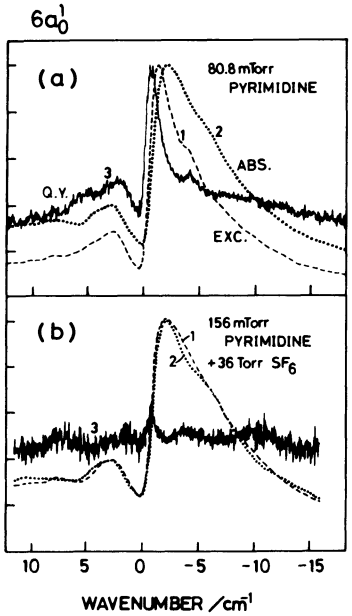

Fig. 2. Spectra for the $6a_0^1$ band of pyrimidine: (1,----) fluorescence excitation spectrum; (2,·····) absorption spectrum; (3,——) fluorescence quantum yield spectrum. Sample vapors: (a) 80.8 mTorr of pyrimidine; (b) 156 mTorr of pyrimidine plus 36 Torr of SF_6. The band origin is denoted by 0.

† 1 Torr≈133.322 Pa.

spectrum gives a prominent peak for excitation frequencies near the band origin, that is, for low values of the total rotational angular momentum quantum number J', the prime referring to the excited state S_1; furthermore, the yield is found to decrease with increasing J'. As is seen in Fig. 2(b), at high pressure, the excitation and absorption spectra agree with each other, giving a flat fluorescence quantum yield spectrum.

Experimental results similar to those given in Figs. 2(a) and 2(b) have been obtained with the 1_0^1 absorption band. Thus, with respect to the rotational-level dependence of fluorescence, the situation in the $6a_0^1$ and 1_0^1 bands is essentially the same as that in the 0-0 band.[13] Note that $\Delta E<1000\ cm^{-1}$ for the $6a^1$ and 1^1 levels.

$6a^2$ Level (ΔE=1291 cm^{-1}). The fluorescence characteristics change in many respects when ΔE becomes higher than 1000 cm^{-1}. Figures 3(a) and 3(b) show fluorescence spectra obtained by excitation at two different positions within the rotational contour of the $6a_0^2$ absorption band of pyrimidine at a low pressure of 80.8 mTorr. In either case, both the IPL and the broad fluorescence appear. However, the fluorescence intensity distribution in Fig. 3(b) is different from the one in Fig. 3(a). In fact, the relative contribution of the IPL fluorescence is larger in Fig. 3(b) than in Fig. 3(a).

Reflecting the change in intensity distribution of the fluorescence spectrum with the rotational level excited, the excitation spectrum at low pressure changes in shape with the region of the fluorescence monitored, as illustrated in Fig. 4. The excitation spectrum in Fig. 4(b), which is related (mainly) to the broad fluorescence, resembles the absorption spectrum more closely than does the excitation spectrum in Fig. 4(a) related to the IPL fluorescence.

The quantum yield spectra for the IPL and broad fluorescence, shown in Figs. 4(a) and 4(b) respectively, vary across the rotational contour of the $6a_0^2$ band with a peak near the band origin. However, the variation of the quantum yield is obviously small in the case of the broad fluorescence. The IPL fluorescence is considered to be involved, to some extent, in the emission at 390 nm, i.e., at the monitoring wavelength in Fig. 4(b). Then the variation of the quantum yield for the broad fluorescence alone should be even smaller than what is seen in Fig. 4(b). It may thus be said that the actual quantum yield of the broad fluorescence will show little or no rotational-level dependence.

Extrapolating spectral data at low pressures, including those given in Fig. 4, to zero pressure, we have reached the conclusion that the broad fluorescence exists even at zero pressure; in other words, the

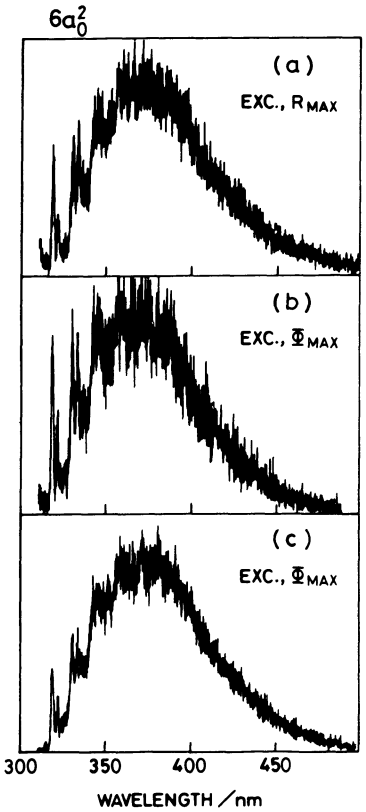

Fig. 3. Fluorescence spectra from the $6a^2$ level of pyrimidine. Sample vapors: (a, b) 80.8 mTorr of pyrimidine; (c) 156 mTorr of pyrimidine plus 36 Torr of SF_6. Excitation positions in the $6a_0^2$ band: (a) maximum of the R branch (R_{max}); (b, c) maximum of the quantum yield spectrum (Φ_{max}).

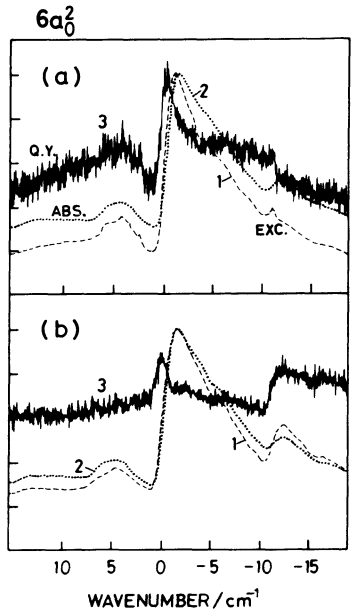

Fig. 4. Spectra for the $6a_0^2$ band of pyrimidine at 80.8 mTorr: (1,----) fluorescence excitation spectrum; (2,·····) absorption spectrum; (3,——) fluorescence quantum yield spectrum. Excitation and quantum yield spectra: (a) obtained by monitoring selectively the IPL fluorescence at 321 nm; (b) obtained by monitoring mainly the broad fluorescence at 390 nm. The band origin is denoted by 0.

broad fluorescence occurs as an intramolecular phenomenon.

Let us now turn to pyrimidine vapor at high total pressure. Figure 3(c) shows the fluorescence spectrum excited at the $6a_0^2$ absorption band of pyrimidine (156 mTorr) in the presence of 36 Torr of SF_6. Here the excitation position corresponds to the maximum of the quantum yield spectrum; it should be noted, however, that the fluorescence spectrum was found to be independent of excitation position within the $6a_0^2$ band. It is seen in Fig. 3(c) that the broad fluorescence appears at high pressure also. The excitation spectra at high pressure (Fig. 5) obtained by monitoring the fluorescence at 321 and 390 nm agree fairly well with the absorption spectrum, so that in both cases the quantum yield spectra are nearly flat over the rotational contour.

Figures 6(a) and 6(b) show the decays of the IPL and broad fluorescence following excitation within the $6a_0^2$ band at a pressure of 80.8 mTorr. The decay curves of Figs. 6(b) and 6(c) were obtained under the same conditions except for the time scales. It is seen from Fig. 6(b) that the broad fluorescence also involves fast and slow components which are analogous to the fast and slow components of the IPL fluorescence found in Fig. 6(a). In each of the IPL and broad fluorescence emissions, the fast and slow components will be called component I and component II, respectively, for the sake of simplicity. Note that, with the time resolution employed in the case of Fig. 6, the photoelectron pulses corresponding to the fast component of fluorescence fall on the first and second channels in (a) and (b), and on the first channel in (c).

The lifetime of the slow component II (τ_{II}) at 80.8 mTorr is found to be 72 ns from Fig. 6(a) for the IPL fluorescence and 81 ns from Fig. 6(b) for the broad fluorescence. Allowing for experimental error, however, the two lifetime values should be regarded as practically equal to each other (vide infra).

The broad fluorescence is thus similar to the IPL fluorescence in the lifetime of component II and also in the ratio of the amount of component I to that of component II. However, as is seen in Fig. 6(c), the broad fluorescence involves another slow component, which will be referred to as component III. The lifetime of component III (τ_{III}) at 80.8 mTorr is about 470 ns, which is much longer than τ_{II} at the same pressure.

The reciprocal lifetimes (τ^{-1}) for components II and III of the broad fluorescence as well as that for component II of the IPL fluorescence are plotted against pressure in Fig. 7. Allowing for experimental error, in the pressure range concerned, one cannot find any appreciable difference in lifetime between

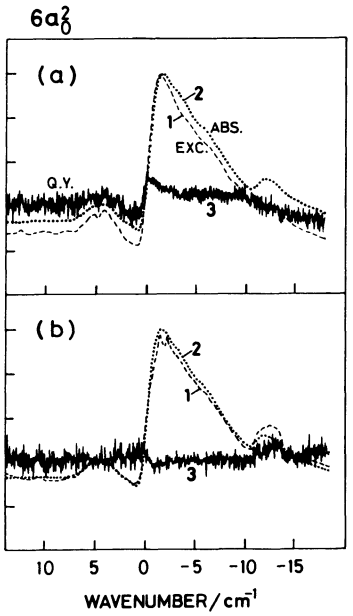

Fig. 5. Spectra for the $6a_0^2$ band of pyrimidine at 156 mTorr in the presence of 36 Torr of SF_6: (1,----) fluorescence excitation spectrum; (2,·····) absorption spectrum; (3,——) fluorescence quantum yield spectrum. Excitation and quantum yield spectra: (a) obtained by monitoring selectively the IPL fluorescence at 321 nm; (b) obtained by monitoring mainly the broad fluorescence at 390 nm. The band origin is denoted by 0.

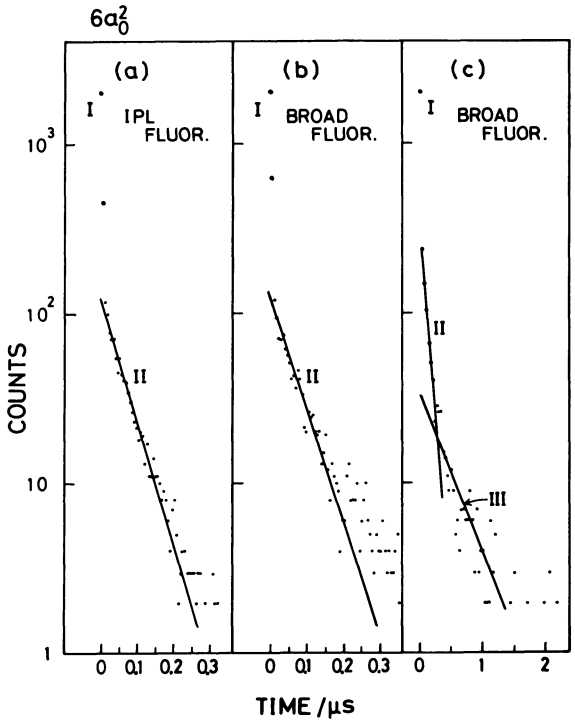

Fig. 6. Fluorescence decays for pyrimidine at 80.8 mTorr after excitation at the maximum of the R branch of the $6a_0^2$ band: (a) obtained by monitoring selectively the IPL fluorescence at 319.5 nm; (b, c) obtained by monitoring mainly the broad fluorescence at 390 nm under the same conditions except for the time scales.

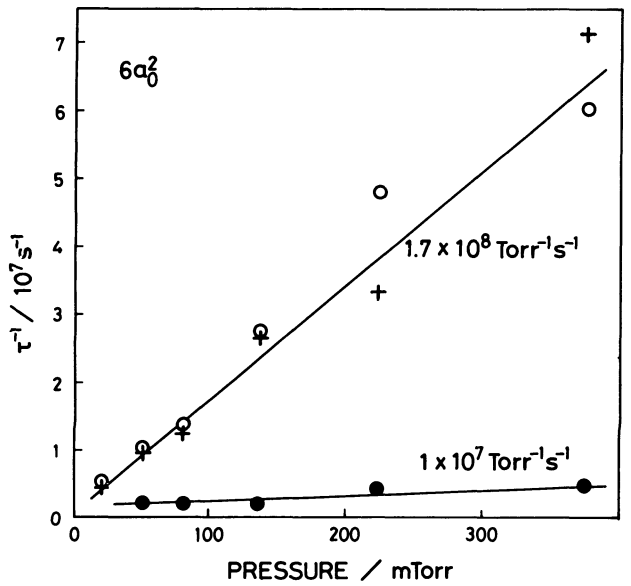

Fig. 7. Plots of τ^{-1} against pressure for $6a^2$ of pyrimidine: O, component II of the IPL fluorescence; +, component II of the broad fluorescence; ●, component III of the broad fluorescence.

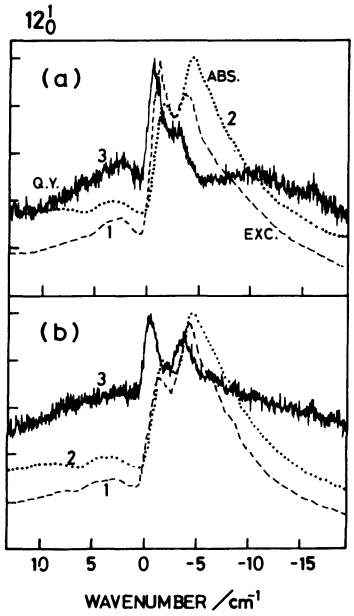

Fig. 8. Spectra for the 12_0^1 band of pyrimidine at 80.8 mTorr: (1,----) fluorescence excitation spectrum; (2,·····) absorption spectrum; (3,——) fluorescence quantum yield spectrum. Excitation and quantum yield spectra: (a) obtained by monitoring selectively the IPL fluorescence at 321 nm; (b) obtained by monitoring mainly the broad fluorescence at 390 nm. The band origin is denoted by 0.

components II of the IPL and broad fluorescence, and these two kinds of components II are quenched in essentially the same manner with increasing pressure. Thus, in either case, the quenching rate constant is evaluated to be about 1.7×10^8 Torr^{-1} s^{-1}, which is more than one order of magnitude larger than the hard sphere collision rate constant ($k_{hsc}\approx1\times10^7$ Torr^{-1} s^{-1}). This indicates that the quenching of components II results from a long-range, weak collision leading to rotational relaxation, as in the case of the slow fluorescence from the 0^0 level.[13]

Component III of the broad fluorescence, on the other hand, is quenched with a rate constant of 1×10^7 Torr^{-1} s^{-1}, which is equal to k_{hsc}. It can thus be said that, among the slow fluorescence components, component III is characterized by a less tendency to undergo collisional quenching. It is to be noted that the lifetime values for components II and III of the broad fluorescence are fairly close to each other at pressures lower than 10 m Torr.

It may be noted here that the occurrence of component I in the decay of the broad fluorescence (Fig. 6) is consistent with the observation that the broad fluorescence exists even at such high pressures that the slower components, II and III, are almost fully quenched.

12^1 Level (ΔE=1012 cm^{-1}). The ΔE value for this level is smaller than that for the $6a^2$ level, but is larger than 1000 cm^{-1}. Figure 8 shows excitation, absorption, and quantum yield spectra for the 12_0^1 band. Actually, the band appears to consist of two overlapping vibronic bands. This situation is clearer in the excitation spectrum obtained under supersonic jet conditions.[20] It is seen from Fig. 8(a) that the quantum yield for the IPL fluorescence varies greatly across the rotational contour. As in the case of the $6a_0^2$ band, the variation of the quantum yield for the broad fluorescence (Fig. 8(b)) is small compared with that for the IPL fluorescence.

The fluorescence decay after excitation into the 12^1 level is similar in nature to the decay after excitation into the $6a^2$ level. The IPL fluorescence and the broad fluorescence decay in similar manners, and both involve components I and II. The lifetimes of components II of the two types of fluorescence are nearly equal to each other at any pressure concerned in the present study. On the other hand, in the case of the 12^1 excitation, component III which is characterized by a less tendency to undergo collisional quenching makes only a negligibly small contribution to the broad fluorescence.

12^2 Level (ΔE=2025 cm^{-1}). Figures 9(a) and 9(b) show, respectively, decay curves for the IPL and broad fluorescence at two different pressures after excitation within the 12_0^2 band. It is seen that the IPL fluorescence consists of components I and II. The broad fluorescence also consists of fast and slow components. The former corresponds to component I. On the other hand, inspection of the decay curves given in Figs. 9(a) and 9(b) clearly shows that the slow component of the broad fluorescence is less liable to be quenched by collisions than component II of the IPL fluorescence,

indicating that the slow component of the broad fluorescence corresponds to component III. Although a small amount of component II can be detected in a decay curve of the broad fluorescence obtained at a higher time resolution, it may be said that the broad fluorescence resulting from excitation into the 12^2 level consists mainly of components I and III. One can thus conclude that the contribution of component III to the broad fluorescence notably increases with increasing ΔE.

The lifetimes of the fast component (component I),

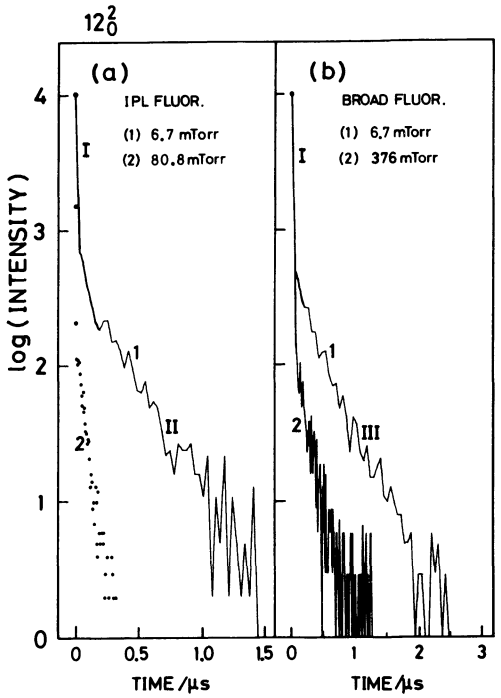

Fig. 9. Fluorescence decays for pyrimidine after excitation at the maximum of the 12^2_0 band: (a) obtained by monitoring the IPL fluorescence at 308.6 nm for (1) 6.7 and (2) 80.8 mTorr of pyrimidine vapor; (b) obtained by monitoring the broad fluorescence at 390 nm for (1) 6.7 and (2) 376 mTorr of pyrimidine vapor.

Table 1. Excess Vibrational Energies (ΔE), Lifetimes of the Fast Component (τ_I) of the IPL and Broad Fluorescence, and k_{SU} for Various Vibronic Levels in S_1 Pyrimidine

Vibronic level	ΔE[a] / cm^{-1}	τ_I/ns IPL	τ_I/ns Broad	k_{SU} / 10^8 s^{-1}
0^0	0			
$6a^1$	613			
1^1	941			
12^1	1012	1.5	2.0	1.7
$6a^2$	1291	0.9	1.3	3.4
$6a^112^1$	1629	1.2	1.4	1.2
12^2	2025	0.8	1.4	5.4
$6a^112^2$	2642			

a) From Refs. 11, 18, and 19.

τ_I, were obtained from decay curves for high-pressure samples by the convolution method. The results are summarized in Table 1 for the IPL and broad fluorescence emitted from some vibronic levels including 12^1, $6a^2$, and 12^2. For any level listed in Table 1, the value of τ_I for the broad fluorescence is larger than the corresponding τ_I value for the IPL fluorescence.

Discussion

The results of the present experiments indicate that the fluorescence of pyrimidine vapor optically excited into an S_1 vibronic level with $\Delta E > 1000$ cm^{-1} involves broad fluorescence besides the IPL fluorescence. Each of the two types of fluorescence gives fast and slow components, I and II. The broad fluorescence gives another slow component, III, which is less liable to undergo collisional quenching than component II; the ratio of the yield of component III to that of component II increases with increasing ΔE.

In the following discussion, we shall give special attention to the mechanism by which the broad fluorescence is generated. It has turned out that general treatment of this subject is mathematically too difficult. Therefore, we first treat three simplified and rather extreme cases on the basis of kinetic schemes shown in Fig. 10. Here, solid and wavy arrows represent radiative (R) and nonradiative (NR) processes, respectively. S is the initially prepared vibronic level (IPL) belonging to S_1. U denotes the emitting levels of the broad fluorescence; it is assumed that these levels also belong to S_1, as will be shown

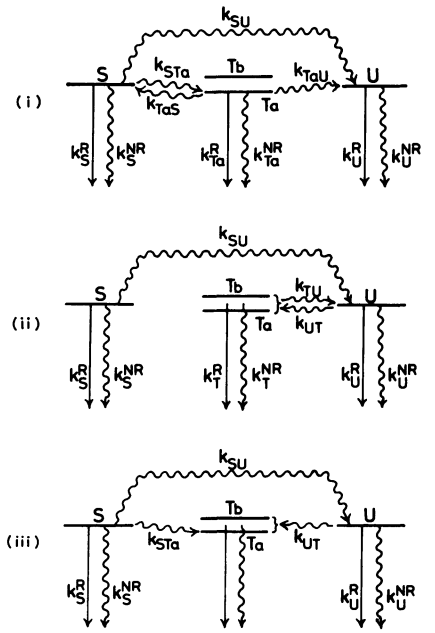

Fig. 10. Kinetic schemes and various rate constants (k) for pyrimidine. R and NR refer to radiative and nonradiative processes, respectively. See text for other symbols.

later. Ta stands for the triplet levels coupled directly to S, and Tb stands for the other triplet levels that are quasidegenerate with S and U. Note that the number of the levels of Ta may be much smaller than the total number of the triplet levels isoenergetic with S and U. The rate constants associated with the individual processes are also given in the figure. For levels with $\Delta E<1000\ \mathrm{cm}^{-1}$, the broad fluorescence is absent, so that we are concerned only with S and Ta.

Case (i). This corresponds to scheme (i) in Fig. 10. In this case, k_{SU} is assumed to be much smaller than k_{STa}. Hence, the population of U will be small in at least the early stage of relaxation, so that the processes U ⇝ Ta, U ⇝ Tb, and Tb ⇝ U are neglected in scheme (i). It is to be noted, however, that the nonradiative rate constant k_U^{NR} is assumed here to include the value of the rate constant which would be associated with U ⇝ T (=Ta+Tb).

According to scheme (i), the concentrations of the molecule existing in the S and U levels, denoted by [S] and [U] respectively, are found to be given, as a function of time t, by

$$[S] = [S]_0\left\{\frac{k_S-\lambda_2}{\lambda_1-\lambda_2}\exp(-\lambda_1 t)+\frac{\lambda_1-k_S}{\lambda_1-\lambda_2}\exp(-\lambda_2 t)\right\}, \tag{1}$$

$$\begin{aligned}[U] = {}& [S]_0\frac{(k_S-\lambda_2)k_{SU}-k_{TaU}k_{STa}}{(\lambda_1-\lambda_2)(k_U-\lambda_1)}\exp(-\lambda_1 t)\\ &+ [S]_0\frac{k_{SU}(k_{Ta}-k_U)+k_{TaU}k_{STa}}{(k_U-\lambda_1)(k_U-\lambda_2)}\exp(-k_U t)\\ &+ [S]_0\frac{(\lambda_1-k_S)k_{SU}+k_{TaU}k_{STa}}{(\lambda_1-\lambda_2)(k_U-\lambda_2)}\exp(-\lambda_2 t),\end{aligned} \tag{2}$$

where

$$\left.\begin{aligned}\lambda_{1,2} &= \frac{1}{2}\{(k_S+k_{Ta})\pm\sqrt{(k_S-k_{Ta})^2+4k_{TaS}k_{STa}}\},\\ k_S &= k_S^R + k_S^{NR} + k_{STa} + k_{SU},\\ k_U &= k_U^R + k_U^{NR},\\ k_{Ta} &= k_{Ta}^R + k_{Ta}^{NR} + k_{TaS} + k_{TaU},\end{aligned}\right\} \tag{3}$$

and $[S]_0$ means [S] at $t=0$; note that $\lambda_1>\lambda_2$. The quantum yield of the IPL fluorescence (Φ_{IPL}) and that of the broad fluorescence (Φ_{broad}) are then expressed as

$$\Phi_{IPL} = \frac{k_S^R k_{Ta}}{k_S k_{Ta}-k_{STa}k_{TaS}} = G^{-1}k_S^R(k_{Ta}^R+k_{Ta}^{NR}+k_{TaS}+k_{TaU}) \tag{4}$$

with

$$\left.\begin{aligned}G &= (k_S^R+k_S^{NR}+k_{STa}+k_{SU})(k_{Ta}^R+k_{Ta}^{NR}+k_{TaU})\\ &\quad + k_{TaS}(k_S^R+k_S^{NR}+k_{SU}),\\ \Phi_{broad} &= \frac{k_U^R}{k_U}\left(\frac{k_{SU}}{k_S^R}\Phi_{IPL}+\frac{k_{TaU}}{k_{Ta}^R}\Phi_{Ta}\right)\end{aligned}\right\} \tag{5}$$

with

$$\Phi_{Ta} = \frac{k_{Ta}^R k_{STa}}{k_S k_{Ta}-k_{STa}k_{TaS}} = G^{-1}k_{Ta}^R k_{STa}. \tag{6}$$

Case (ii). This corresponds to scheme (ii) in Fig. 10. In this case, it is assumed that $k_{STa} \ll k_{SU}$, and the interaction between S and Ta is neglected accordingly. The nonradiative rate constant k_S^{NR}, however, is assumed here to include the value of the rate constant which would be associated with S ⇝ Ta. Note that in scheme (ii) U is considered to interact with both Ta and Tb. Thus, in Fig. 10, T represents collectively all the triplet levels belonging to Ta and Tb.

According to scheme (ii), [S] and [U] are given by

$$[S] = [S]_0\exp(-k_S t), \tag{7}$$

$$\begin{aligned}[U] = {}& [S]_0\frac{\alpha}{k_{UT}}\left\{(k_T-k_S)\exp(-k_S t)\right.\\ &+ \frac{(k_T-\gamma_1)(\gamma_2-k_S)}{\gamma_1-\gamma_2}\exp(-\gamma_1 t)\\ &\left.+ \frac{(k_T-\gamma_2)(k_S-\gamma_1)}{\gamma_1-\gamma_2}\exp(-\gamma_2 t)\right\},\end{aligned} \tag{8}$$

where

$$\left.\begin{aligned}\gamma_{1,2} &= \frac{1}{2}\{(k_U+k_T)\pm\sqrt{(k_U-k_T)^2+4k_{UT}k_{TU}}\},\\ k_S &= k_S^R + k_S^{NR} + k_{SU},\\ k_T &= k_T^R + k_T^{NR} + k_{TU},\\ k_U &= k_U^R + k_U^{NR} + k_{UT},\\ \alpha &= \frac{k_{UT}k_{SU}}{(k_S-\gamma_1)(k_S-\gamma_2)}.\end{aligned}\right\} \tag{9}$$

Note that $\gamma_1>\gamma_2$.

Case (iii). This corresponds to scheme (iii) in Fig. 10. In this case, processes Ta ⇝ S and T ⇝ U are neglected.

According to scheme (iii), [S] and [U] are given by

$$[S] = [S]_0\exp(-k_S t), \tag{10}$$

$$[U] = [S]_0\frac{k_{SU}}{k_S-k_U}\{-\exp(-k_S t)+\exp(-k_U t)\} \tag{11}$$

Here, only the fast fluorescence emissions occur. The quantum yields for the fast components of the IPL fluorescence and broad fluorescence, denoted by Φ_{IPL}^I and Φ_{broad}^I respectively, are given by

$$\Phi_{IPL}^I = k_S^R/k_S, \tag{12}$$

$$\Phi_{broad}^I = \frac{k_U^R}{k_U}\frac{k_{SU}}{k_S}. \tag{13}$$

In Eqs. 10—13, k_S and k_U are defined as

$$\left.\begin{aligned}k_S &= k_S^R + k_S^{NR} + k_{STa} + k_{SU},\\ k_U &= k_U^R + k_U^{NR} + k_{UT}.\end{aligned}\right\} \tag{14}$$

Interpretation of Experimental Results at Low Pressure. Using the kinetic schemes presented in Fig. 10, we first discuss the results of experiments made at low pressure.

Let us first consider case (i). According to Eq. 1, the IPL fluorescence gives fast and slow components, I

and II, with lifetimes $1/\lambda_1$ and $1/\lambda_2$, respectively. It may be noted that $1/\lambda_1<1/\lambda_2$, since $\lambda_1>\lambda_2$. Let us assume here that in Eq. 2

$$\lambda_1>k_U>\lambda_2. \tag{15}$$

It can then be shown that in Eq. 2 the preexponential factor for $\exp(-\lambda_1 t)$ is negative, but that the factors for $\exp(-k_U t)$ and $\exp(-\lambda_2 t)$ are both positive. Therefore, Eq. 2 indicates that the broad fluorescence should give a biexponential decay preceded by a rise. It is natural to consider that $1/k_U$ is the lifetime of component I. The third term on the right hand side of Eq. 2 decays with a lifetime of $1/\lambda_2$ which is equal to the lifetime of component II of the IPL fluorescence, so that the third term in question can be assigned to component II of the broad fluorescence. Thus, the dynamics of pyrimidine excited into the 12^1 level corresponds closely to case (i). The behavior of pyrimidine after excitation into the $6a^2$ level can be described by case (i), except that component III appears weakly upon $6a^2$ excitation. It may be noted that component III does not occur in case (i); it results from reversible intersystem crossing between U and T(=Ta+Tb), as seen in scheme (ii) of Fig. 10. To sum up, aside from component III mentioned above, case (i) accounts for our observations that (1) the broad fluorescence resulting from the excitation into $6a^2$ or 12^1 level shows at least approximately a biexponential decay similar to the one of the IPL fluorescence and (2) the lifetimes of components II of the broad fluorescence and the IPL fluorescence agree with each other. However, we could not detect the rise portion in the change in intensity of the broad fluorescence with time. It may be noted that the assumption of inequalities (15) is considered to be valid, because $\lambda_1>k_S$ and moreover k_U would be smaller than k_S by a value corresponding to k_{SU} (see Table 1), and because λ_2 is of the order of the reciprocal lifetime of the triplet state.

Most of the fluorescence properties of pyrimidine that are observed after 12^1_0 or $6a^2_0$ excitation can be explained, at least approximately or qualitatively, in terms of case (i) by assuming that only the rate constant k_{TaS} depends on the rotational level excited. It is reasonable to consider that, in Eq. 4, $k_{STa} \gg k_S^R+k_S^{NR}+k_{SU}$ and that k_{TaS} is comparable in magnitude to $k_{Ta}^R+k_{Ta}^{NR}+k_{TaU}$. The factor G will then be insensitive to the variation of k_{TaS}. One may thus expect that Φ_{IPL} given by Eq. 4 is an approximately linear function of k_{TaS}. According to Eq. 6, on the other hand, Φ_{Ta} is insensitive to the variation of k_{TaS}, so that it follows from Eq. 5 that there is a linear relation between Φ_{broad} and k_{TaS}. Owing to the existence of the constant term, $k_U^R k_{TaU}\Phi_{Ta}/k_U k_{Ta}^R$, Φ_{broad} varies with k_{TaS} to a lesser extent than does Φ_{IPL}. Thus, the rotational level dependence of the quantum yield of the broad fluorescence (Φ_{broad}) at low pressure would be small compared with that of the IPL fluorescence (Φ_{IPL}) in agreement with our observation.

We now proceed to the fluorescence emissions from the 12^2 and $6a^112^2$ levels at low pressure. Suppose here that case (ii) holds true. Then it follows from Eq. 7 that the IPL fluorescence lacks component II. Further, since one can assume that $k_{SU} \gg k_S^R+k_S^{NR}$, Φ_{IPL} should be much smaller than Φ_{broad}. On the assumption that

$$k_S>\gamma_1>k_T>\gamma_2, \tag{16}$$

it can readily be verified that the broad fluorescence is characterized by a rise due to $-\exp(-k_S t)$, a fast decay (component I) due to $\exp(-\gamma_1 t)$ and a slow decay due to $\exp(-\gamma_2 t)$ (see Eq. 8). This slow decay is attributable to component III, since the quenching rate constant of component III is expected to be much smaller than that of component II, as will be seen later. It is to be noted that component III associated with case (ii) results from reversible intersystem crossing between U and T which includes the triplet levels uncoupled to S (see γ_2 in Eq. 9). On the other hand, component II of the broad fluorescence associated with case (i) results from reversible intersystem crossing between S and Ta which is directly coupled to S (see λ_2 in Eq. 3). Thus, in case (ii), the broad fluorescence consists of components I and III without involving component II.

The foregoing considerations indicate that the dynamics of pyrimidine excited into the $6a^112^2$ level just corresponds to case (ii). For excitation into the 12^2 level, the dynamics appears to be close to case (ii), but the observed IPL fluorescence from 12^2 includes component II as well as I (Fig. 9(a)). Therefore, the relaxation processes from 12^2 cannot fully be explained by case (ii).

Interpretation of Experimental Results at High Pressure. At high pressures where the slower components II and III are fully quenched, leaving the fast component I free from the collisional perturbation, the recurrence from Ta and/or Tb to S and/or U can be neglected, because the collision-induced vibrational relaxation in the triplet state is to be very fast. Consequently, for any initially excited level leading to the broad fluorescence, the situation at high pressure may be described in terms of case (iii).

According to Eq. 10, the IPL fluorescence shows an exponential decay due to $\exp(-k_S t)$, which is associated with the fast component I. Equation 11 indicates that the broad fluorescence also shows an exponential decay due to $\exp(-k_U t)$, associated with component I; in this case, however, the decay is preceded by a rise due to $-\exp(k_S t)$.

As will be mentioned later, U is assigned to rovibronic levels belonging to S_1 and isoenergetic with S. It may then be assumed, though very roughly, that

$$k_S^R + k_S^{NR} + k_{STa} \approx k_U^R + k_U^{NR} + k_{UT}. \tag{17}$$

It follows from Eqs. 14 and 17 that

$$k_S - k_U \approx k_{SU}. \quad (18)$$

As expected from this relation, the observed lifetime of component I (τ_I) of the IPL fluorescence, $1/k_S$, is shorter than the corresponding lifetime of the broad fluorescence, $1/k_U$, for all the excited vibronic levels studied (see Table 1). These lifetime data enable one to obtain approximate values of k_{SU} from Eq. 18. The resulting k_{SU} values are given in Table 1, from which it is seen that k_{SU} ranges in magnitude from 10^8 to 10^9 s^{-1} in the ΔE range 1000—2000 cm^{-1}. It may be noted that the rise of the broad fluorescence, which is predicted from Eq. 11, could not be detected with the present time resolution.

Behavior of Component III. As has been mentioned in the section of results, there is a substantial difference in rate of collisional quenching between component II and component III. In fact, the quenching rate constants for components II of the IPL fluorescence and broad fluorescence are ten times as large as k_{hsc}, whereas that for component III of the broad fluorescence is nearly equal to k_{hsc}. It is to be recalled here that the slow component of the (IPL) fluorescence from lower vibronic levels of intermediate-case molecules,[13,14] including pyrimidine, is known to have a quenching rate constant much larger than k_{hsc}.

According to a quantum-mechanical treatment of the behavior of intermediate-case molecules,[10,11,21] the slow fluorescence components, II and III, are emitted from mixed levels that result from coupling of singlet and triplet levels. In terms of the kinetic model, the same coupling is described by reversible conversion between the singlet and triplet levels,[21] as shown in Fig. 10 with forward and backward wavy arrows. Note that U is here assumed to represent singlet levels.

Let us first consider the collisional quenching of component II of the IPL fluorescence. This component originates from S–Ta mixed levels. At a lower vibronic level S, prepared initially, the singlet rovibronic level density is low. Hence a weak collision can transfer pyrimidine molecule from the S–Ta mixed levels to pure triplet rovibronic levels, which are not coupled to any singlet level, resulting in quenching of the IPL fluorescence.[11] At a high vibronic level S, such as 12^2 or $6a^112^2$, the singlet rovibronic level density is very high. Hence, there is a large probability that a weak collision will transfer the molecule from the S–Ta mixed levels to triplet rovibronic levels which are coupled to singlet levels. However, even if the latter rovibronic levels may give emission, the emission must be different from the IPL fluorescence. Accordingly, in this case also, the IPL fluorescence itself is quenched by a weak collision. It should be noted in this connection that, when we were concerned with the behavior of the IPL fluorescence, we measured its intensity by monitoring selectively an appropriate peak in the IPL fluorescence spectrum. From the foregoing discussion it can be concluded that, whether the initially prepared vibronic level S is low or high, the IPL fluorescence is quenched very efficiently with a rate much greater than that of the hard sphere collision.

Since component II of the broad fluorescence is closely associated with component II of the IPL fluorescence (see scheme (i) in Fig. 10), the former component II is also expected to undergo efficient collisional quenching as in the case of the latter.

Now, component III, which originates from U–T mixed levels, appears in the broad fluorescence from the pyrimidine molecule excited into its higher vibronic levels, such as 12^2 and $6a^112^2$. At these levels, the singlet rovibronic level density is so high that only a hard collision that can remove an energy of hundreds of cm^{-1} will transfer the molecule from the U–T mixed levels to pure triplet levels and thereby will quench component III. This accounts for the observation that, unlike component II, component III has as small a collisional quenching constant as k_{hsc}. In the above argument, the following has been assumed implicitly: When the pyrimidine molecule undergoes collisional transfer (owing to a weak collision) from the U–T mixed levels to other triplet levels with singlet character, the fluorescence from the latter levels is similar in spectral shape and position to, and hence indistinguishable from, component III of the broad fluorescence emitted from the U–T mixed levels; apparently, therefore, the collisional transfer in question does not lead to quenching of component III.

Mention should be made here of a study by Spears and El-Manguch[11] on the dual fluorescence of pyrimidine vapor. On the basis of the pressure dependence of the fluorescence decay, these authors reported that the collisional quenching constant of the slow component of fluorescence is remarkably smaller for higher vibronic levels (12^2 and $6a^112^2$) than for lower levels (0^0, $6a^1$, 12^1, and $6a^112^1$), and that the higher levels have quenching constants close (or equal) to k_{hsc}. They interpreted these experimental results in terms of the energy level dependence of the singlet level density in much the same way as we have done in our discussion. In the study by Spears and El-Manguch, however, the total fluorescence was monitored, with no attention being given to the fact that the fluorescence from pyrimidine vapor may contain not only the IPL fluorescence but also the broad fluorescence in our definition. In their experiments on the higher levels (12^2 and $6a^112^2$), the observed slow emission should be regarded as consisting largely of component III of the broad fluorescence.

Spears and El-Manguch[11] reported also that the

behavior of pyrimidine fluorescence observed when the pressure is increased up to 0.5 Torr is unusual. On excitation to vibronic levels higher than $6a^1$, they observed varying degrees of nonexponential decay for the slow component of fluorescence in the pressure range 0.1—0.5 Torr. Especially for excitation to the 12^2 and $6a^112^2$ levels, the increase in pressure to 0.5 Torr causes the appearance of a large background that appears to be flat over the time scale of the experiment.

The above observations by Spears and El-Manguch can readily be understood by taking account of component III of the broad fluorescence. As the pressure is increased, component II is quenched to a far greater extent than is component III, so that the amount of III may become comparable or superior to the amount of II. This leads to the nonexponential decay of the slow fluorescence or to the appearance of the background, which can be assigned naturally to component III.

Intramolecular Vibrational Redistribution (IVR). It was suggested in our previous papers[14,22] that in the case of 1,3,5-triazine the emitting levels of the broad fluorescence, U, are those vibronic levels which belong not only to S_1 but also to another singlet electronic state. This is rationalized by the observation that the radiative rate constant of the 1,3,5-triazine molecule increases with increasing excess vibrational energy.[22] On the contrary, in pyrimidine the radiative rate constant is largest for the 0^0 level and it decreases roughly monotonically with increasing excess energy.[19] One may thus reasonably assign U to S_1 vibronic levels which are isoenergetic with S. In other words, the conversion from S to U corresponds to the IVR, which is considered to occur in pyrimidine vapor not only directly from S but also via triplet levels.

For the fluorescence from the 12^2 level of pyrimidine, Lim et al.[16] reported experimental results similar to ours. On the basis of their experiments on the bulk gas and on a supersonic jet,[16] they pointed out that the fluorescence spectrum of pyrimidine vapor excited into its 12^2 level consists of a subspectrum with a sharp spectral feature and a subspectrum with a broad feature. The former was attributed to resonance fluorescence from the 12^2 level and the latter to fluorescence from levels which are populated through IVR. Furthermore, they found, as we did, that the excitation spectra with respect to the two fluorescence subspectra are different from each other in shape. This, along with temperature dependence of the characteristics of the subspectra, led them to the conclusion that the IVR process shows rotational level dependence which is to be predicted from the Coriolis interaction. Thus, their conclusion agrees with ours in the sense that the broad fluorescence is emitted from levels populated through IVR, but it is discrepant from our view concerning the nature of the IVR.

The data available in the present experiments indicate that, at high pressure, the quantum yields of the IPL and broad fluorescence emissions obtained by excitation at a vibronic band are independent of the rotational level excited. This means that $\Phi^{\mathrm{I}}_{\mathrm{IPL}}$ and $\Phi^{\mathrm{I}}_{\mathrm{broad}}$ are constant irrespective of the rotational level, since only the fast fluorescence components survive at high pressure. The quantum yields of the fast components, $\Phi^{\mathrm{I}}_{\mathrm{IPL}}$ and $\Phi^{\mathrm{I}}_{\mathrm{broad}}$, are given by Eqs. 12 and 13. For any vibronic level, the radiative rate constants $k^{\mathrm{R}}_{\mathrm{S}}$ and $k^{\mathrm{R}}_{\mathrm{U}}$ can reasonably be regarded as independent of the rotational level. Then the constancy of $\Phi^{\mathrm{I}}_{\mathrm{IPL}}$ ensures that k_{S} is independent of the rotational level (Eq. 12). This along with the constancy of $\Phi^{\mathrm{I}}_{\mathrm{broad}}$ indicates that $k_{\mathrm{SU}}/k_{\mathrm{U}}$ also is independent of the rotational level (Eq. 13). The rate constant k_{U} defined by Eq. 14 seems to be independent of the rotational level. Furthermore, it is hardly conceivable that k_{SU} and k_{U} vary with the rotational level in the same manner so that the ratio $k_{\mathrm{SU}}/k_{\mathrm{U}}$ may become constant. It can be concluded, therefore, that k_{SU} as well as k_{U} does not depend appreciably on the rotational level excited.

In their work already mentioned,[16] Lim et al. interpreted their observation of rotational contour dependence of the fluorescence of pyrimidine by presuming that Coriolis coupling plays an important role in IVR. According to these authors, the rate constant of IVR is governed by a factor $\sqrt{J(J+1)-K(K+1)}$, which appears in the matrix element of the second-order Coriolis interaction. Note that the pyrimidine molecule is here regarded as a symmetric top, and that J and K are the rotational quantum numbers. In other words, the rate constant k_{SU} (in our notation) should depend strongly on the rotational level belonging to S in marked contrast to our conclusion.

We have already shown in Fig. 9 the fluorescence decays of pyrimidine after excitation at the 12^2_0 band. It is seen in Fig. 9(a) that the IPL fluorescence contains the slow component, II. The content of component II is found to be about 15 percent of the total IPL fluorescence at 80.8 mTorr, which pressure is close to the one employed by Lim et al. in their experiment on the bulk gas. If we take account of this observation and of the fact that the yield of the slow component of the IPL fluorescence varies with the rotational level excited, then on the assumption that k_{SU} is independent of the rotational level we are able to explain most of the experimental results reported by Lim et al. We, therefore, believe that the rate of the IVR does not depend on the rotational level; in other words, the Coriolis coupling plays no significant role in the IVR process.

Up to now, the occurrence of IVR has been noticed

for many molecules.[1-4] Almost all of these molecules, however, belong to the statistical limit case, where the fluorescence is characterized by a single exponential decay. Except for 1,3,5-triazine,[14,22] pyrimidine is the first example of the intermediate case molecule in which IVR has been found to occur. It is worthy of note that the IVR in pyrimidine is observed even for levels with small excess vibrational energies ($\approx$1000 cm^{-1}). In a statistical limit case molecule with a size similar to benzene and with no side chain, IVR is observed usually for levels with excess energies of more than $\approx$2000 cm^{-1}.[5,6] For some alkylbenzenes[4,7] the IVR is observed for levels with very small excess energies such as 530 cm^{-1}. However, these molecules have low frequency modes like the torsion or the bending of the alkyl chain, so that the situation in alkylbenzenes is different from that in pyrimidine. Using the vibrational frequencies in the literature,[18] the vibronic state density of pyrimidine at ΔE=1000 cm^{-1} in S_1 was found to be as small as $\approx$0.06 cm from the Haarhoff formula.[23] It should be reasonable, therefore, to consider that the rotational levels will cause the effective state density to increase and thereby will be involved in the IVR occurring in S_1 pyrimidine.

This work was partly supported by a Grant-in-Aid for Cooperative Research (58340028) from the Ministry of Education, Science and Culture.

References

1) K. F. Freed and A. Nitzan, *J. Chem. Phys.*,**73**, 4765 (1980), and references cited therein.

2) P. R. Stannard and W. M. Gelbert, *J. Phys. Chem.*,**85**, 3592 (1981), and references cited therein.

3) C. S. Parmenter, *J. Phys. Chem.*, **86**, 1735 (1982), and references cited therein.

4) R. E. Smalley, *J. Phys. Chem.*, **86**, 3504 (1982), and references cited therein.

5) M. Sumitani, D. V. O'Connor, Y. Takagi, N. Nakashima, K. Kamogawa, Y. Udagawa, and K. Yoshihara, *Chem. Phys.*, **93**, 359 (1985).

6) R. A. Coveleskie, D. A. Dolson, and C. S. Parmenter, *J. Chem. Phys.*, **72**, 5774 (1980); D. A. Dolson, C. S. Parmenter, and B. M. Stone, *Chem. Phys. Lett.*, **81**, 360 (1981).

7) J. B. Hopkins, D. E. Powers, S. Mukamel, and R. E. Smalley, *J. Chem. Phys.*, **72**, 5049 (1980).

8) J. B. Hopkins, D. E. Powers, and R. E. Smalley, *J. Chem. Phys.*, **73**, 683 (1980); H. T. Jonkman and D. A. Wiersma, *Chem. Phys. Lett.*, **97**, 261 (1983); S. A. Schwartz and M. R. Topp, *Chem. Phys.*, **86**, 245 (1984).

9) E. Riedle, H. J. Neusser, and E. W. Schlag, *J. Phys. Chem.*, **86**, 4847 (1982); E. Riedle, H. J. Neusser, E. W. Schlag, and S. H. Lin, *J. Phys. Chem.*, **88**, 198 (1984).

10) K. Uchida, I. Yamazaki, and H. Baba, *Chem. Phys. Lett.*, **38**, 133 (1976); *Chem. Phys.*, **35**, 91 (1978).

11) K. G. Spears and M. El-Manguch, *Chem. Phys.*, **24**, 65 (1977).

12) H. Baba, M. Fujita, and K. Uchida, *Chem. Phys. Lett.*, **73**, 425 (1980).

13) H. Baba, N. Ohta, O. Sekiguchi, M. Fujita, and K. Uchida, *J. Phys. Chem.*, **87**, 943 (1983), and references cited therein.

14) N. Ohta and H. Baba, *Chem. Phys.*, **82**, 41 (1983).

15) D. M. Bartels and K. G. Spears, *J. Phys. Chem.*, **86**, 5180 (1982); H. Saigusa and E. C. Lim, *Chem. Phys. Lett.*, **88**, 455 (1982); *J. Chem. Phys.*, **78**, 91 (1983).

16) B. E. Forch, K. T. Chen, H. Saigusa, and E. C. Lim. *J. Phys. Chem.*, **87**, 2280 (1983); K. T. Chen, B. E. Forch, and E. C. Lim, *Chem. Phys. Lett.*, **99**, 98 (1983); B. E. Forch and E. C. Lim, *Chem. Phys. Lett.*, **110**, 593 (1984).

17) H. Baba, M. Fujita, N. Ohta, and Y. Shindo, *J. Spectrosc. Soc. Jpn.*, **29**, 387 (1980).

18) A. E. W. Knight, C. M. Lawburgh, and C. S. Parmenter, *J. Chem. Phys.*, **63**, 4336 (1975).

19) I. Yamazaki, M. Fujita, and H. Baba, *Chem. Phys.*, **57**, 431 (1981).

20) O. Sekiguchi, N. Ohta, and H. Baba, unpublished data.

21) F. Lahmani, A. Tramer, and C. Tric, *J. Chem. Phys.*, **60**, 4431 (1974).

22) N. Ohta and H. Baba, *Chem. Phys. Lett.*, **106**, 382 (1984); **112**, 212 (1984).

23) P. C. Haarhoff, *Mol. Phys.*, **7**, 101 (1963).